



## CHAPTER II

### LITERATURE REVIEW

#### 2.1 Theoretical Background

##### 2.1.1 Epoxidation Reaction

The epoxidation of olefin is an important reaction for in the industrial production of several compounds, as well as for the synthesis of many intermediates, useful chemicals, and pharmaceuticals. The epoxidation of olefin results in oxygenated molecules, so-called epoxide, by oxygen transfer reaction.

An epoxide is cyclic ether with three ring atoms. This ring can be approximately defined as an equilateral triangle, which makes it highly strained. The strained ring makes epoxides more reactive than other ethers. The formation of epoxide is shown in Figure 2.1.

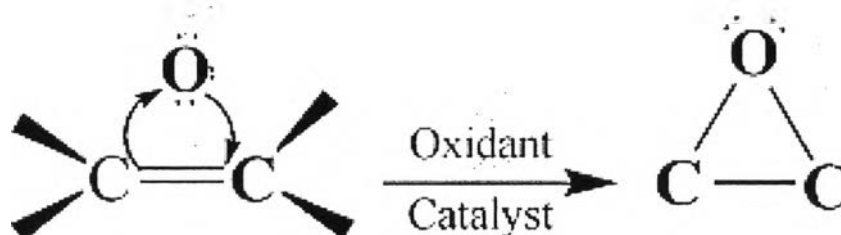


**Figure 2.1** The formation of epoxide from alkene.

An oxidant is required to accomplish this transformation. The molecular oxygen is the most desirable oxidant for epoxidation because of its availability and low cost. In addition, hydrogen peroxide ( $\text{H}_2\text{O}_2$ ) and *tert*-butyl hydroperoxide (TBHP) can be used as the oxidant. In many cases,  $\text{H}_2\text{O}_2$  is preferentially selected because it is easy to handle and possess relatively high active oxygen content (Oyama *et al.*, 2008).

## 2.1.2 Types of Epoxidation Reaction

### 2.1.2.1 *Jacobsen-Katsuki Epoxidation*

The Jacobsen-Katsuki epoxidation allows the enantioselective formation of epoxides from various *cis*-substituted olefins by using a chiral Mn-salen catalyst and a stoichiometric oxidant, such as bleach. As compared to the Sharpless epoxidation, the Jacobsen-Katsuki epoxidation allows a broader substrate scope for the transformation; good substrates are conjugated *cis*-olefins (R: Ar, alkenyl, alkynyl; R': Me, alkyl) or alkyl-substituted *cis*-olefins bearing one bulky alkyl group. The Jacobsen-Katsuki epoxidation is shown in Figure 2.2.

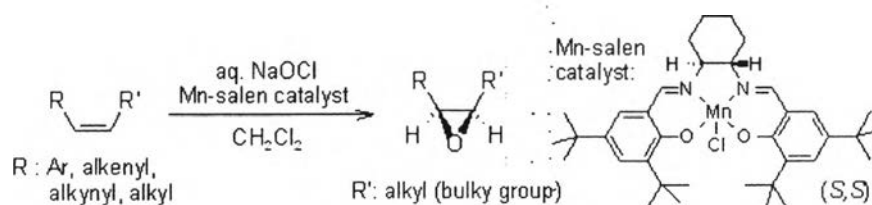


**Figure 2.2** The formation of epoxide from Jacobsen-Katsuki epoxidation.

### 2.1.2.2 *Prilezhaev Epoxidation*

The epoxidation of an alkene with peracid gives an oxirane. The commercially available 3-chloroperoxybenzoic acid (mCPBA) is a widely used reagent for this conversion, while magnesium mono-perphthalate and peracetic acid are also employed. The Prilezhaev epoxidation is shown in Figure 2.3.

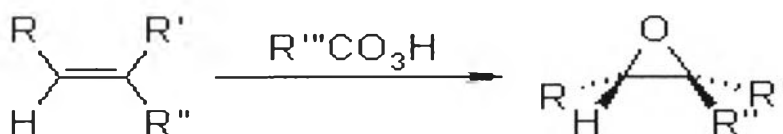


**Figure 2.3** The formation of epoxide from Prilezhaev epoxidation.

### 2.1.2.3 Sharpless Epoxidation

The Sharpless epoxidation allows the enantioselective epoxidation of prochiral allylic alcohols. The asymmetric induction is achieved by adding an enantiomerically enriched tartrate derivative. The Sharpless epoxidation is shown in Figure 2.4.

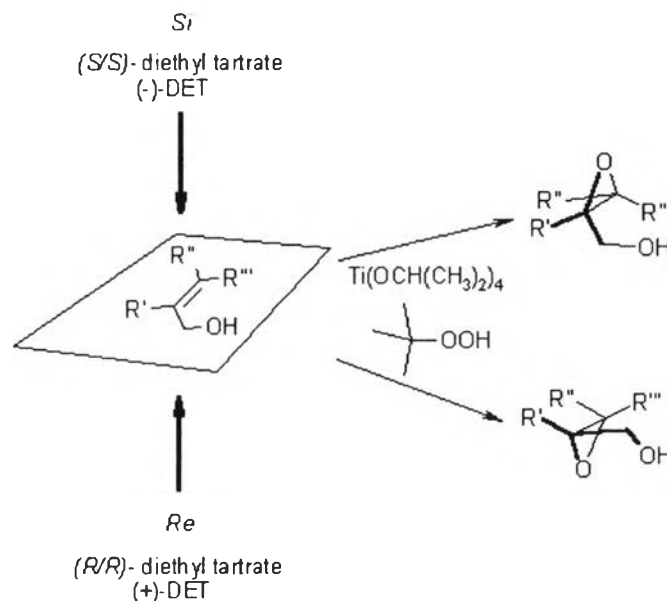
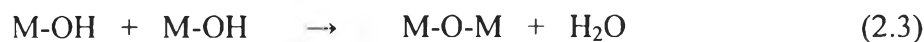


**Figure 2.4** The formation of epoxide from Sharpless epoxidation.

### 2.1.3 Sol-Gel Method

Several key techniques have been adopted to prepare mesoporous materials, such as sol-gel process, hydrothermal process, and ultrasonic irradiation process. The sol-gel process is one of the versatile methods to prepare nano-sized mesoporous materials (Sreethawong *et al.*, 2005). This technique does not require complicated instruments, such as in chemical vapor deposition method. It provides a simple and easy means of synthesizing nano-sized particles, which is essential for nano-catalysts (Wu and Chen, 2004). Besides, it is capable of producing catalysts with a high surface area. It involves the formation of metal-oxo-polymer network from molecular precursors, such as metal alkoxides, and subsequent polycondensation as follows:



where M = Ti, Si, Zr, Al, and R = alkyl group. The relative rates of hydrolysis and polycondensation strongly influence the structure and properties of the resulting metal oxides. Typically, sol-gel-derived precipitates are amorphous in nature, requiring further heat treatment to induce crystallization. The calcination process frequently gives rise to particle agglomeration and growth and may induce phase transformation (Wang and Ying, 1999).

Factors affecting the sol-gel process include the reactivity of metal alkoxides, pH of the reaction medium, water-to-alkoxide ratio, reaction temperature, and nature of solvent and additive. The water-to-alkoxide ratio governs the sol-gel chemistry and the structural characteristics of the hydrolyzed gel. High water-to-alkoxide ratio in the reaction medium ensures a more complete hydrolysis of alkoxides, favoring nucleation versus particle growth. In addition, an increase in water-to-alkoxide ratio leads to reducing the crystallite size of the calcined catalyst. An alternative approach to control the sol-gel reaction rates involves the use of acid or base catalyst. It was reported that for a system with a water-to-alkoxide ratio of 165, the addition of HCl resulted in the reduction of the crystallite size from 20 to 14 nm for materials calcined at 450 °C. Besides, a finer grain size and a narrower pore size distribution with a smaller average pore diameter were also attained for the sample synthesized with HCl (Wang and Ying, 1999). The size of alkoxide group in alkoxides also plays an important role in controlling the particle size. The titanium alkoxide containing bulky groups, such as titanium amiloxide, reduces the hydrolysis rate, which is advantageous for the preparation of fine colloidal particles (Murakami *et al.*, 1999).

#### 2.1.4 Support Material for Epoxidation Reaction

##### 2.1.4.1 *Titanium Dioxide or Titania (TiO<sub>2</sub>)*

The reducible metal oxide is one of the most important supports, which provide a strong metal-support interaction (SMSI), particularly TiO<sub>2</sub>

support. It has been known that  $\text{TiO}_2$  exhibits a strong metal-support interaction effect with group VIII noble metals.

$\text{TiO}_2$  is an n-type semiconductor and a typical photocatalyst, attracting much attention from both fundamental and practical viewpoints. It has been used in many industrial areas, including environmental purification, solar cells, gas sensors, pigments, and cosmetics. To explore novel approaches for the nanostructured  $\text{TiO}_2$ , the control of the particle size in nanometer-scale and the morphology is quite interesting, since the performance of  $\text{TiO}_2$  in various applications depends on its crystalline phase state, dimensions, and morphology.

$\text{TiO}_2$  is a lustrous silver-white metal oxide that occurs naturally in three crystalline polymorphs: anatase (tetragonal), rutile (tetragonal), and brookite (orthorhombic). The last one is, however, not common. Rutile is the thermally stable form at all temperatures, but conversion of anatase to rutile is so slow that it may be unimportant in most catalytic reactions. Anatase typically has a higher surface area than rutile.  $\text{TiO}_2$  with surface areas in the range of about  $10 \text{ m}^2/\text{g}$  to  $50 \text{ m}^2/\text{g}$  (Degussa P-25) is commercially available. Typically, fumed  $\text{TiO}_2$  consists of mixture of anatase and rutile, with the ratio varying somewhat with the manufacturing process. Degussa P-25 is reported to contain about 85 to 90 % anatase and 10 to 15 % rutile (Satterfield, 1991).

For nanocrystalline mesoporous  $\text{TiO}_2$ , it generally possesses high catalytic efficiency because of its unique properties conferred by very small physical dimensions. The large specific surface area and high volume fraction of atoms located both on the surface and at the grain boundaries result in an increased surface energy. Then, the surface of nanocrystalline mesoporous  $\text{TiO}_2$  provides an active substrate for catalysis. In addition, the reactants are operated across the porous system in several catalytic applications. Sufficiently uniform pore size between 2 nm and 50 nm in the mesoporous region is more suitable if loading of cocatalysts/dopants is required as not to become easily blocked as in the case of microporous materials (pore size  $< 2 \text{ nm}$ ). Therefore, the surface of nanocrystalline  $\text{TiO}_2$  particles with a mesoporous structural network is more promising because catalytic activity can be further enhanced due to the enlarged surface area for

facilitating better reactant accessibility to the catalyst surfaces and subsequent surface reactions (Sreethawong *et al.*, 2006).

#### 2.1.4.2 Cerium (IV) Oxide ( $CeO_2$ )

$CeO_2$  is an oxide of the rare earth metal cerium.  $CeO_2$  can be formed by calcining cerium (IV) diammonium nitrate,  $(NH_4)_2Ce(NO_3)_6$ .  $CeO_2$  is the most stable phase at room temperature and under atmospheric conditions.  $CeO_2$  is generally used in ceramics, to sensitize photosensitive glass, as a catalyst and a catalyst support, and to polish glass and stones. It is also used in the walls of self-cleaning ovens as a hydrocarbon catalyst during the high-temperature cleaning process. While it is transparent for visible light, it absorbs ultraviolet radiation strongly. So, it is a prospective replacement of ZnO and  $TiO_2$  in sunscreens.

$CeO_2$  has been used in catalytic converters in automotive applications. Since  $CeO_2$  can become non-stoichiometric in oxygen content depending on its ambient partial pressure of oxygen, it can release or take in oxygen in the exhaust stream of a combustion engine. In association with other catalysts,  $CeO_2$  can effectively reduce  $NO_x$  emissions, as well as convert harmful carbon monoxide to the less harmful carbon dioxide.  $CeO_2$  is particularly interesting for catalytic conversion economically because it has been shown that adding comparatively inexpensive  $CeO_2$  can allow for substantial reductions in the amount of platinum needed for complete oxidation of  $NO_x$  and other harmful products of incomplete combustion. Due to its fluorite structure, the oxygen atoms in a  $CeO_2$  crystal are all in a plane with one another, allowing for rapid diffusion as a function of the number of oxygen vacancies. As the number of vacancies increases, the ease at which oxygen can move around in the crystal increases, allowing the  $CeO_2$  to reduce and oxidize molecules or co-catalysts on its surface. It has been shown that the catalytic activity of  $CeO_2$  is directly related to the number of oxygen vacancies in the crystal, frequently measured by using XPS to compare the ratios of  $Ce^{3+}$  to  $Ce^{4+}$  in the crystal (Deshpande *et al.*, 2005).  $CeO_2$  can also be used as a co-catalyst in a number of reactions, including the water-gas shift and steam reforming of ethanol or diesel fuel into hydrogen gas and carbon dioxide (with varying combinations of rhodium oxide, iron oxide, cobalt oxide, nickel oxide, platinum, and gold), the Fischer-Tropsch reaction, and selected oxidation (particularly with lanthanum). In

each case, it has been shown that increasing the CeO<sub>2</sub> oxygen defect concentration results in increased catalytic activity, making it very interesting as a nanocrystalline co-catalyst due to the heightened number of oxygen defects as crystallite size decreases. At very small sizes, as many as 10 % of the oxygen sites in the fluorite structure crystallites will be vacancies, resulting in exceptionally high diffusion rates.

## 2.2 Literature Review

The epoxidation of olefin to epoxide is an important reaction because epoxides can be transformed into useful chemicals. Epoxide is normally used as the raw material for a wide variety of products owing to the numerous reactions they may undergo. Moreover, several epoxides find a range of applications in pharmaceutical industry as drug intermediates, preparation of epoxy resins, perfumes, pesticides, and paints

Mendellin *et al.* (2001) studied the epoxidation of cyclohexene and cyclooctene by using  $\text{Al}_2\text{O}_3$  as a simple catalyst for the epoxidation, because it was inexpensive and safe, and using anhydrous hydrogen peroxide as an oxidant. Productivity of up to 4.3 g product per g catalyst was obtained, and the catalyst could be recycled without significant loss of activity. Moreover, the reaction mechanism of the  $\text{Al}_2\text{O}_3$ -catalyzed alkene epoxidation was proposed in Figure 2.5.

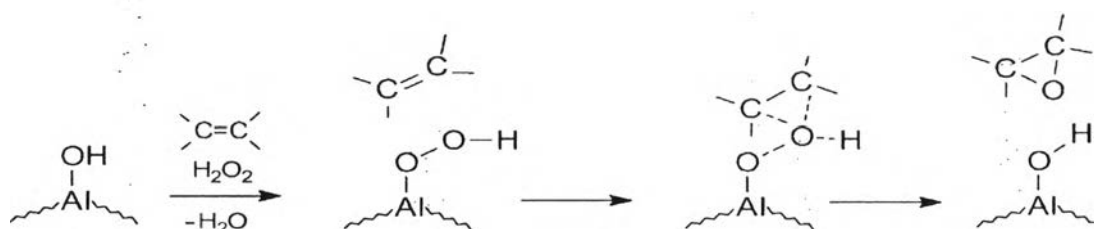


**Figure 2.5** Proposed mechanism for the  $\text{Al}_2\text{O}_3$ -catalyzed alkene epoxidation (Mandelli *et al.*, 2001).

Kanai *et al.* (2003) studied the selective epoxidation of allyl acetate with *tert*-butyl hydroperoxide (TBHP) over the group IV-VI metal oxide supports, namely  $\text{SiO}_2$ ,  $\text{Al}_2\text{O}_3$ , and  $\text{TiO}_2$ . The epoxidation required higher temperature than those of electron-donating olefin did. The highest yield of epoxide was achieved over  $\text{MoO}_3/\text{TiO}_2$  with an adequate  $\text{MoO}_3$  loading, which was determined so that the surface of  $\text{TiO}_2$  was two-dimensionally and fully covered with  $\text{MoO}_3$ .

Fraile *et al.* (2003) studied the optimization of cyclohexene epoxidation using dilute hydrogen peroxide and silica-supported titanium catalysts. The type of silica support, the silanization with long hydrocarbon chains, and the slow addition



of hydrogen peroxide were found to be important factors. Silica-supported titanium species were efficient catalysts for the epoxidation. The silanization of the silica surface and titanium dispersion had positive effects on yield, selectivity, and recoverability of the catalyst, showing the role of the radical pathway in deactivation and titanium leaching. In the best case, the catalyst could be reused at least three times with very low titanium leaching, and an overall productivity of 228 mmol epoxidation products per mmol Ti was achieved. The reaction pathways of the cyclohexene epoxidation were proposed, as shown in Figure 2.6.

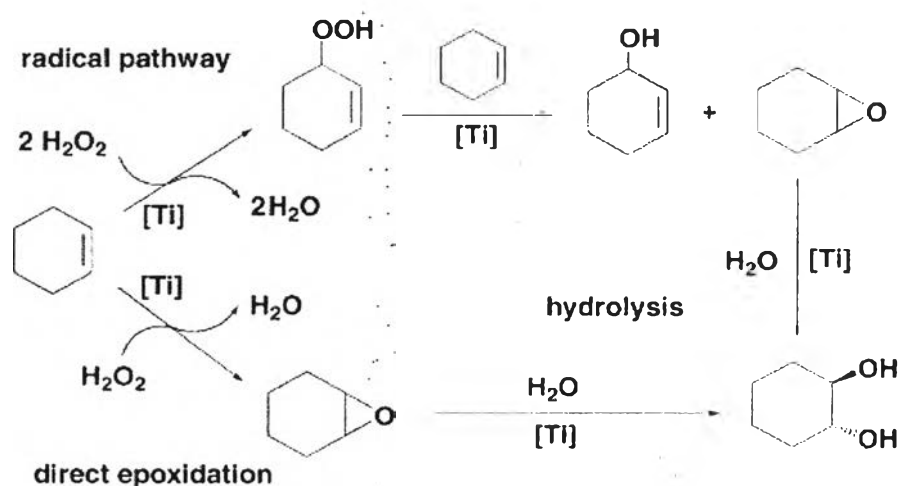


**Figure 2.6** Reaction pathways in the epoxidation of cyclohexene with dilute hydrogen peroxide (Fraile *et al.*, 2003).

Sreethawong *et al.* (2005) prepared nanocrystalline mesoporous  $\text{TiO}_2$ -based catalysts by a surfactant-assisted templating sol-gel process, which were used for epoxidation of cyclohexene in *tert*-butanol- $\text{H}_2\text{O}_2$  system. The mesoporous  $\text{TiO}_2$  showed both higher cyclohexene conversion and higher cyclohexene oxide selectivity than non-mesoporous commercial  $\text{TiO}_2$ . The oxides of Fe, Co, Ni, and Ru were also loaded by the incipient wetness impregnation method onto the synthesized mesoporous  $\text{TiO}_2$ , aiming to increase the catalytic performance.  $\text{RuO}_2$ -loaded mesoporous  $\text{TiO}_2$  was found to possess noticeably high catalytic performance based on cyclohexene oxide selectivity. The 1 mol%  $\text{RuO}_2$ -loaded mesoporous  $\text{TiO}_2$  was the best catalyst, showing the highest cyclohexene oxide selectivity (desired product)

and lowest cyclohex-2-en-1-ol (undesired product). In addition, the possible reaction pathway and the active species formed in the cyclohexene epoxidation were proposed, as shown in Figure 2.7.

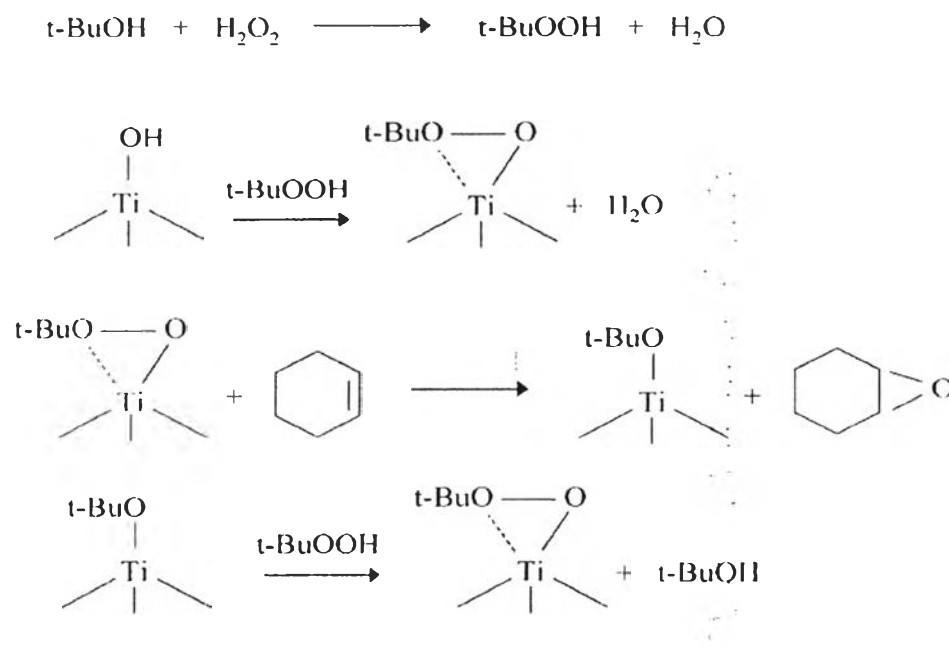


**Figure 2.7** Proposed pathway for cyclohexene epoxidation at TiO<sub>2</sub> surface (Sreethawong *et al.*, 2005).

Sreethawong *et al.* (2006) continued to further optimize reaction conditions for cyclohexene epoxidation with H<sub>2</sub>O<sub>2</sub> over nanocrystalline mesoporous TiO<sub>2</sub> loaded with RuO<sub>2</sub>. The TiO<sub>2</sub> support prepared by a surfactant-assisted templating sol-gel process was nanocrystalline and had mesoporous structure with narrow monomodal pore size distribution. The 1 mol% of RuO<sub>2</sub> was loaded on the synthesized TiO<sub>2</sub> by the incipient wetness impregnation method. The reaction conditions in the epoxidation reaction, namely reaction temperature, amount of catalyst, and concentration of H<sub>2</sub>O<sub>2</sub> in terms of cyclohexene/H<sub>2</sub>O<sub>2</sub> ratio, were systematically optimized to obtain a maximum selectivity for cyclohexene oxide.

Waragamon *et al.* (2010) studied the liquid-phase cyclohexene epoxidation with H<sub>2</sub>O<sub>2</sub> over RuO<sub>2</sub>-loaded mesoporous-assembled TiO<sub>2</sub> nanocrystals. The RuO<sub>2</sub>-loaded mesoporous-assembled TiO<sub>2</sub> was prepared by both the incipient wetness

impregnation method ( $\text{RuO}_2/\text{TiO}_2$  (IWI)) and single-step sol-gel method ( $\text{RuO}_2/\text{TiO}_2$  (SSSG)). The 1 mol%  $\text{RuO}_2/\text{TiO}_2$  (SSSG) calcined at 450 °C showed high cyclohexene conversion and cyclohexene oxide selectivity. The recyclability of  $\text{RuO}_2/\text{TiO}_2$  (IWI) and  $\text{RuO}_2/\text{TiO}_2$  (SSSG) catalysts was also studied. It was found that after three consecutive catalytic reaction cycles, the  $\text{RuO}_2/\text{TiO}_2$  (IWI) exhibited a slight decrease in cyclohexene conversion, but cyclohexene oxide selectivity decreased significantly. On the contrary, the  $\text{RuO}_2/\text{TiO}_2$  (SSSG) exhibited no changes in both cyclohexene conversion and cyclohexene oxide selectivity, indicating its much higher stability. In addition, XRF and TPR were used to test the strong metal oxide-support interaction. The results revealed that the  $\text{RuO}_2/\text{TiO}_2$  (SSSG) possessed a higher stability due to a stronger metal oxide-support interaction.

Reddy *et al.* (2010) investigated the epoxidation of cyclohexene using aqueous hydrogen peroxide over  $\text{Fe}/\text{CeO}_2$  catalysts prepared by co-precipitation. The catalytic activity and main product selectivity were found to strongly depend on catalyst composition, acidity, and reducibility. Cyclohexene epoxide and 1,2-cyclohexanediol were found to be the main products. The effect of varying the concentrations of Fe on  $\text{CeO}_2$  was investigated. A high cyclohexene conversion rate of 99 mol% and an epoxide selectivity of 98 mol% were observed over the 5 %  $\text{Fe}/\text{CeO}_2$  at 100 °C. The aggregate iron oxide species was revealed in the case of the 20 %  $\text{Fe}/\text{CeO}_2$  catalyst. The reducibility of the  $\text{CeO}_2$  upon Fe doping and the increase in the number of acid sites were obtained in the case of Fe doping up to 5 %. The highly dispersed iron oxide on  $\text{CeO}_2$  was found in the 2 %  $\text{Fe}/\text{CeO}_2$  and 5 %  $\text{Fe}/\text{CeO}_2$  catalysts, whereas for the 10 %  $\text{Fe}/\text{CeO}_2$  and 20 %  $\text{Fe}/\text{CeO}_2$  catalysts, aggregates of Fe species were observed.